
Erik Jonsson School of Engineering and Computer Science

2015-1

*Deformation Potentials for Band-To-Band Tunneling
in Silicon and Germanium from First Principles*

UTD AUTHOR(S): William G. Vandenberghe and Massimo V. Fischetti

©2015 AIP Publishing LLC

Vandenberghe, W. G., and M. V. Fischetti. 2015. "Deformation potentials for band-to-band tunneling in silicon and germanium from first principles." *Applied Physics Letters* 106(1): doi:10.1063/1.4905591.

Deformation potentials for band-to-band tunneling in silicon and germanium from first principles

William G. Vandenberghe and Massimo V. Fischetti

Department of Materials Science and Engineering, The University of Texas at Dallas,
 800 W Campbell Rd. RL10, Richardson, Texas 75080, USA

(Received 28 October 2014; accepted 24 December 2014; published online 8 January 2015)

The deformation potentials for phonon-assisted band-to-band tunneling (BTBT) in silicon and germanium are calculated using a plane-wave density functional theory code. Using hybrid functionals, we obtain: $D_{TA} = 4.1 \times 10^8$ eV/cm, $D_{TO} = 1.2 \times 10^9$ eV/cm, and $D_{LO} = 2.2 \times 10^9$ eV/cm for BTBT in silicon and $D_{TA} = 7.8 \times 10^8$ eV/cm and $D_{LO} = 1.3 \times 10^9$ eV/cm for BTBT in germanium. These values agree with experimentally measured values and we explain why in diodes, the TA/TO phonon-assisted BTBT dominates over LO phonon-assisted BTBT despite the larger deformation potential for the latter. We also explain why LO phonon-assisted BTBT can nevertheless dominate in many practical applications. © 2015 AIP Publishing LLC. [<http://dx.doi.org/10.1063/1.4905591>]

Tunneling from valence band to conduction band, also known as Band-to-Band tunneling (BTBT) or Zener tunneling, has generated great interest in the last decade and is expected to play an important role in future nanotransistors. BTBT is both important in metal-oxide field-effect transistors (MOSFETs), the current work-horse of the semiconductor industry, and in tunnel field-effect transistors (TFETs),^{1–3} a possible successor of the MOSFET. In MOSFETs, BTBT is responsible for gate-induced drain leakage (GIDL) and the reduction of GIDL is a major concern when charge retention is important.⁴ In TFETs, BTBT is responsible for the TFET drive current as well as the parasitic leakage currents limiting the TFET off-current. To be able to understand device working and to optimize device design, a good model of BTBT is required.

In the semiclassical picture, BTBT can be modeled as the non-local generation or recombination of carriers. The generation rate can be computed from Kane's model,^{5–8} which can be written as a function of the electric field (\mathcal{E})

$$G = A\mathcal{E}^C \exp(-B/\mathcal{E}) \quad (1)$$

with A , B , and C material-dependent parameters with $C = 2$ for direct semiconductors and $C = 2.5$ for indirect semiconductors. The Kane model parameters can either be obtained by fitting the Kane model with experimental data or by performing a theoretical calculation. The parameters obtained from a fitting procedure often have great uncertainty because it is very difficult to determine the active doping profile up to nanometer precision.⁹ This makes theoretical calculations very valuable.

In direct semiconductors, the electronic bandstructure completely determines the parameters,⁸ but in indirect semiconductors, the conduction-band minimum and valence-band maximum occur at different places in the Brillouin zone and crystal momentum can only be conserved when an additional scattering process mediates the BTBT. The dominant intrinsic BTBT-mediating interaction in indirect semiconductors is the electron-phonon interaction, and the BTBT-rate will also be determined by the energy of the phonon mediating

the transition and by the strength of the interaction, measured by a deformation potential. Unfortunately, apart from crude estimates,^{10–12} few attempts have been made to compute the electron-phonon deformation potentials for BTBT in technologically important materials.¹³ Recently, however, advances in computational speed and algorithms have made it possible to calculate electron-phonon interaction strengths from first principles.^{14–16}

In this paper, we compute the deformation potentials for phonon-assisted band-to-band tunneling in silicon and germanium. First, we derive how the deformation potential can be calculated from the phonon displacement vectors, the electronic wavefunctions, and the potential energy of the crystal calculated using density functional theory (DFT). Next, we use the Vienna *ab initio* simulation package (VASP)¹⁷ to compute these physical quantities. Finally, we present the calculated deformation potentials, how the largest deformation potential not always results in the largest tunneling probability, and we end with our conclusion.

Comparing to our initial results for graphene and silicon presented in Ref. 18, the current manuscript presents (i) a derivation and a correction of the expression to calculate the deformation potentials, (ii) the calculation of the deformation potentials in germanium, (iii) the calculation of the deformation potentials using hybrid functionals, (iv) an analysis of the impact of symmetry on the tunneling probability, and (v) reconciliation and comparison with experimental results.^{9,11}

To first order in the ion displacement, the electron-phonon interaction Hamiltonian is

$$H_{e-ph} = \sum_{jl} \frac{\partial H_e}{\partial \mathbf{R}_{jl}} \cdot \delta \mathbf{R}_{jl} \approx \sum_{jl} \frac{\partial U(\mathbf{r})}{\partial \mathbf{R}_{jl}} \cdot \delta \mathbf{R}_{jl}, \quad (2)$$

where H_e is the electron Hamiltonian, \mathbf{R}_{jl} is the position of the ion in unit cell j with l the index labeling each ion in the unit cell, $U(\mathbf{r})$ is the potential energy part of the electron Hamiltonian, and $\partial U(\mathbf{r})/\partial \mathbf{R}_{jl}$ is the gradient of the potential energy with respect to the displacement of ion jl . The ion displacement operator is given by

$$\delta \mathbf{R}_{jl} = \sum_{\mathbf{q}} d_{\mathbf{q}l}^{\nu} \mathbf{e}_{\mathbf{q}l}^{\nu} e^{i\mathbf{q} \cdot \mathbf{R}_{jl}} [a_{\mathbf{q}}^{\nu} + a_{-\mathbf{q}}^{\nu\dagger}] \quad (3)$$

with $a_{\mathbf{q}}^{\nu}$ and $a_{\mathbf{q}}^{\nu\dagger}$ are the annihilation and creation operators for a phonon in branch ν with wavevector \mathbf{q} and a frequency $\omega_{\mathbf{q}}^{\nu}$, with $\mathbf{e}_{\mathbf{q}l}^{\nu}$ is the phonon unit displacement vectors, and

$$d_{\mathbf{q}l}^{\nu} = \sqrt{\frac{\hbar}{2NM_l\omega_{\mathbf{q}}^{\nu}}} \quad (4)$$

is the magnitude of the ion displacement. Finally, M_l is the mass of ion l and N is the number of unit cells in the lattice.

The matrix element associated with a process in which an electron starting in band n with wavevector \mathbf{k} makes a transition to band m and wavevector $\mathbf{k} + \mathbf{q}$, while emitting a phonon is given by

$$\begin{aligned} \langle m\mathbf{k} + \mathbf{q} | H_{e-\text{ph}} a_{\mathbf{q}}^{\nu\dagger} | n\mathbf{k} \rangle \\ = \sum_{jl} d_{\mathbf{q}l}^{\nu} e^{i\mathbf{q} \cdot \mathbf{R}_{jl}} \mathbf{e}_{\mathbf{q}l}^{\nu} \cdot \left(\int_{\Omega} d\mathbf{r}^3 \psi_{m\mathbf{k}+\mathbf{q}}^*(\mathbf{r}) \frac{\partial U_{\text{H}}(\mathbf{r})}{\partial \mathbf{R}_{0l}} \psi_{n\mathbf{k}}(\mathbf{r}) \right), \end{aligned} \quad (5)$$

where the wavefunctions $\psi_{m\mathbf{k}}(\mathbf{r}) = u_{m\mathbf{k}}(\mathbf{r}) e^{i\mathbf{k} \cdot \mathbf{r}}$ are Bloch functions and their periodic part $u_{m\mathbf{k}}(\mathbf{r})$ is normalized on the unit-cell.

The quantity generally used to measure the strength of the electron-phonon interaction is the deformation potential $DK_{nm\mathbf{k}\mathbf{q}}^{\nu}$. This can be related to the electron-phonon matrix element as

$$\langle m\mathbf{k} + \mathbf{q} | H_{e-\text{ph}} a_{\mathbf{q}}^{\nu\dagger} | n\mathbf{k} \rangle = \frac{1}{\sqrt{\Omega}} \sum_{\nu} DK_{nm\mathbf{k}\mathbf{q}}^{\nu} \sqrt{\frac{\hbar}{2\rho\omega_{\mathbf{q}}^{\nu}}} \quad (6)$$

where $\rho = M_{\text{cell}}/\Omega_{\text{cell}}$ is the mass density, M_{cell} is the mass of the unit cell, Ω_{cell} is the volume of the unit cell, and $\Omega = N\Omega_{\text{cell}}$ is the total volume of the structure. Combining Eqs. (5) and (6), the deformation potential can be calculated as

$$DK_{\mathbf{k}\mathbf{q}mn}^{\nu} = \sum_l \mathbf{M}_{mn\mathbf{k}\mathbf{q}l} \cdot \mathbf{e}_{\mathbf{q}l}^{\nu} \sqrt{\frac{M_{\text{cell}}}{M_l}}, \quad (7)$$

where

$$\mathbf{M}_{mn\mathbf{k}\mathbf{q}l} = \int_{\Omega} d\mathbf{r}^3 u_{m\mathbf{k}+\mathbf{q}}^*(\mathbf{r}) \frac{\partial U(\mathbf{r})}{\partial \mathbf{R}_l} u_{n\mathbf{k}}^*(\mathbf{r}) e^{i\mathbf{q} \cdot (\mathbf{R}_l - \mathbf{r})}. \quad (8)$$

To compute the deformation potentials using Eqs. (7) and (8), the phonon displacement vectors, the gradient of the potential energy with respect to the ion displacement and the wavefunctions are required. We obtain all of these quantities from the charge density in the ground state for silicon and germanium. The gradient of the potential energy is calculated as a finite difference between the potential energy calculated assuming the ions slightly displaced from their equilibrium position in different directions. The ground-state charge density is found by performing a minimization of the density functional using the plane-wave DFT computer package VASP, as mentioned above.

Unless specified, otherwise, we use the Perdew-Burke-Ernzerhof (PBE) functional for the exchange correlation, we take an energy cut-off of 600 eV, a $11 \times 11 \times 11$ Monkhorst-Pack grid and a convergence threshold of 10^{-6} eV. When using the hybrid functionals, we use the HSE06 functional with a $4 \times 4 \times 4$ Monkhorst-Pack grid.

The phonon properties of the structure are obtained by the small-displacement method: The forces acting on the ions are calculated upon a small displacement of each ion. The set of forces can be converted into the force constants, which are required to construct the dynamical matrix. The eigenvalues of the dynamical matrix are the phonon frequencies, while the eigenvectors are the phonon displacement vectors. We use the PHONOPY package to generate a set of $3 \times 3 \times 3$ supercells with displaced atoms, to compute the force constants, and to diagonalize the dynamical matrix.

The potential energy is obtained as the Hartree part of the Kohn-Sham Hamiltonian used in VASP. Displacing each atom from its equilibrium position ($\mathbf{R}_l^{(0)}$) in each direction $\alpha = x, y, z$ in the unit cell to a position $\mathbf{R}_l^{(0)} + \delta_{\alpha}$, the gradient of the potential energy with respect to atom displacement can be obtained using finite differences

$$\left[\frac{\partial U(\mathbf{r})}{\partial \mathbf{R}_{0l}} \right]_{\alpha} \approx \frac{U_{\text{H}}(\mathbf{r})|_{\mathbf{R}_l=\mathbf{R}_l^{(0)}+\delta_{\alpha}} - U_{\text{H}}(\mathbf{r})|_{\mathbf{R}_l=\mathbf{R}_l^{(0)}-\delta_{\alpha}}}{2|\delta_{\alpha}|}. \quad (9)$$

We note that, in contrast to the rigid-ion approximation,^{19–21} the screening of the ion potential by the valence electrons is automatically accounted for in the DFT-based approach.

For the wavefunctions, we take the Kohn-Sham wavefunctions for the unit cell, where each atom is in its equilibrium position. We transform the wavefunctions from reciprocal to real space by performing an inverse Fourier transform onto the grid used for the potential energy. We assume the pseudo-wavefunctions are a good description of the real wavefunctions for the purpose of calculating the deformation potentials.

Calculating the Si bandstructure using VASP, the conduction band minimum occurs along the Δ -direction, which is in accordance with silicon's well-known indirect bandgap. But as is expected from DFT, the bandgap is underestimated and the simulated indirect bandgap is only 0.6 eV, while the experimentally measured bandgap is 1.12 eV. Employing the HSE06 hybrid functional on the other hand, the simulated bandgap is 1.19 eV, which is much closer to the experimental bandgap.

There is a first caveat in our numerical procedure to calculate the deformation potential related to the choice of the real-space grid \mathbf{r} . In Eq. (8), the integration is taken over the volume of the entire lattice Ω , but numerically it is satisfactory to integrate over a small volume since the gradient of the potential energy is screened by the valence electrons and quickly decays away from the atom that is being moved. Calculating the matrix element over a single and over multiple unit cells, we find an integration over a single unit cell is satisfactory provided the coordinates are chosen such that $\mathbf{r} = \mathbf{R}_l$ lies at the center of the unit cell.

A second caveat is related to the degeneracy of the initial electronic states ($m\mathbf{k}$), the final electronic states ($n\mathbf{k} + \mathbf{q}$), or the phonon branches ($\nu\mathbf{q}$). In case of degeneracy, the band or branch index is not sufficient to determine the state uniquely

and simply writing the deformation between conduction band and valence band as “ D_{cvkq}^ν ” is ambiguous. For example, the valence band at Γ is three-fold degenerate in absence of spin-orbit coupling and the different wavefunctions rotate like p_x , p_y , and p_z orbitals. For the phonons, the TA and the TO phonons are degenerate: if we take the phonon wavevector along the x -direction, the transverse phonon displacements will lie in the y - z plane. So depending on which linear combination of the valence band wavefunctions is taken and the direction of the phonon displacement vectors, different values for “ D_{cvkq}^ν ” are obtained. We remove this ambiguity without spending the effort to symmetrize the different degenerate wavefunctions and polarization vectors: we define the deformation potential between valence and conduction band D_{cvkq}^ν as the largest deformation potential upon rotation of the wavefunctions and phonon displacement vectors in the subspace of the degeneracies. Numerically, D_{cvkq}^ν can be obtained by constructing a tensor out of the deformation potentials of the different degenerate bands and phonon branches and taking the largest multilinear singular value.²² For our calculations, we looked at valence band and phonon branch degeneracies and an ordinary singular value decomposition was satisfactory to calculate our deformation potentials.

Fig. 1 shows the calculated deformation potential for an electron starting at the top of the valence band making a transition to the lowest conduction band. The results shown in Fig. 1 are a correction of our previous results in Ref. 18 because we had erroneously omitted the phase factor $e^{iq \cdot (\mathbf{R}_i - \mathbf{r})}$ in Eq. (8). The deformation potentials relevant for BTBT are found at 0.85 in the Γ -X direction, and their calculated values are $D_{\text{TA}} = 3.5 \times 10^8$ eV/cm, $D_{\text{TO}} = 1.0 \times 10^9$ eV/cm, and $D_{\text{LO}} = 2.3 \times 10^9$ eV/cm. These values are much larger than previous theoretical estimates,¹⁰ but this is in line with the recent experimental estimate $D_{\text{TO}} \approx 10 - 13 \times 10^8$ eV/cm from Ref. 9.

Employing the HSE06 hybrid functional to calculate the wavefunctions, we obtain instead $D_{\text{TA}} = 4.1 \times 10^8$ eV/cm, $D_{\text{TO}} = 1.2 \times 10^9$ eV/cm, and $D_{\text{LO}} = 2.2 \times 10^9$ eV/cm. The hybrid functional reduces the LO deformation potential and increases the TA and the TO phonon interaction strength but the

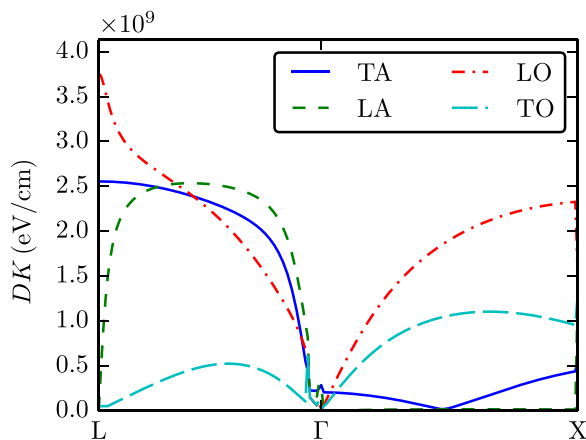


FIG. 1. Silicon deformation potentials for tunneling from the top of the valence band towards the conduction band calculated from VASP using the PBE functional. For BTBT, the values are taken at 0.85 in the Γ -X direction and measure $D_{\text{TA}} = 3.5 \times 10^8$ eV/cm, $D_{\text{TO}} = 1.0 \times 10^9$ eV/cm, and $D_{\text{LO}} = 2.3 \times 10^9$ eV/cm.

LO phonon deformation potential remains the largest. To explain why experimental results in Ref. 11 convincingly show that the LO-mediated process is much weaker than the processes mediated by the TO phonons, we have to consider that the BTBT transition probability ($w \propto D^2 T$) depends not only on the deformation potentials (D) but also on the tunnel probability (T).

Along the 100 (Δ) direction, the O_h Si symmetry group reduces to C_{4v} and the conduction band has Δ_1 symmetry, while the upper (heavy) valence band is two-fold degenerate and has Δ_5 symmetry and the lower (light) valence band has Δ'_2 symmetry.^{23,24} For the phonons, the LA has Δ_1 symmetry, the LO has Δ'_2 symmetry and the TA and the TO have Δ_5 symmetry. Whether a phonon can enable a transition between bands is determined by whether the matrix element transforms as a scalar under the different symmetry operations, or, in group theory, if the direct product of the symmetry groups of the phonon and the initial and final electronic states contains the identity representation (Δ_1 in our case). As an example, transitions between the Δ'_2 valence band and the conduction band, cannot be mediated by an LA phonon since $\Delta'_2 \otimes \Delta_1 \otimes \Delta_1 = \Delta'_2$. Overall, transitions cannot be mediated by the LA phonon, the LO phonon connects the Δ'_2 valence band to the conduction band and the TA/TO phonons connect the Δ_5 valence band to the conduction band.

For tunneling, electrons with light masses will have reduced wavefunction attenuation in the bandgap and their tunneling probability will be increased with respect to those with heavy masses. For the Si conduction band valley, the longitudinal electron mass is much larger than the transversal electron mass making tunneling along the transversal direction favorable. The Δ'_2 valence band has its light mass in the longitudinal direction and will be heavy along the transversal directions, while the Δ_5 valence bands have their light hole masses along the transversal directions. From a tunneling perspective, the transition from the Δ_5 to the conduction band is favored. So while the deformation potential of the LO phonon is higher compared to that of the TA and the TO phonon, its tunneling probability is much smaller making the BTBT transition probability $w_{\text{LA,TO}} > w_{\text{LO}}$.

Spin-orbit interaction and interactions with higher bands warp the valence bands but the energy scale of these effects is small compared to the bandgap and these effects will not enable the LO to significantly couple the valence to the conduction band. However, if tunneling occurs along an axis different from the $\langle 100 \rangle$ direction such as the $\langle 111 \rangle$ direction, the tunneling probabilities for the LO and the TO/TA will have similar orders of magnitude and the transition probability of the LO will dominate because of its larger deformation potential. Furthermore, if strain or quantum confinement²⁵ lift the degeneracy between the six silicon conduction band valleys, the LO phonon can also dominate.

For germanium, the calculated deformation potential values at the L symmetry point are $D_{\text{TA}} = 8.1 \times 10^8$ eV/cm and $D_{\text{LO}} = 1.2 \times 10^9$ eV/cm using the PBE functionals and $D_{\text{TA}} = 7.8 \times 10^8$ eV/cm and $D_{\text{LO}} = 1.3 \times 10^9$ eV/cm using the HSE06 functionals with calculated phonon frequencies $\hbar\omega^{\text{TA}} = 6$ meV and $\hbar\omega^{\text{LO}} = 31$ meV. The phonon frequencies are similar to those found experimentally²⁶ but the deformation potentials are much larger than our previous crude estimates $D_{\text{TO,prev}} = 0.8 \times 10^8$ eV/cm in Ref. 8.

In germanium, the conduction band minimum occurs at the L-point which has D_{3d} symmetry. The conduction band has L_1 symmetry, the TA, LA, LO, and TO phonons have L_3 , L'_2 , L_1 , and L'_3 symmetry, respectively, and the valence band states at Γ are compatible with a L_1 (Λ_1 , light along $[111]$) and a L_3 (Λ_3 , heavy along $[111]$) symmetry representation. The TA and the LO phonon enable BTBT from the L_3 and the L_1 valence band, respectively. In the same way, TO phonons dominate over LO phonons in silicon, TA-assisted BTBT will dominate over LO-assisted BTBT when the field is perpendicular to the $\langle 111 \rangle$ direction despite the larger deformation potential for the LO interaction.

In conclusion, using density functional theory, the deformation potentials can be calculated from the phonon displacement vectors, the gradient of the potential with respect to ion displacement, and the wavefunctions. For silicon BTBT, we found $D_{TA} = 4.1 \times 10^8$ eV/cm, $D_{TO} = 1.2 \times 10^9$ eV/cm, and $D_{LO} = 2.2 \times 10^9$ eV/cm using the HSE06 functional, similar to the deformation potentials we calculated using the PBE functionals. In previous experimental measurements, the LO phonon contribution to BTBT was found to be small, we have shown that this is because the LO phonon couples the Δ'_2 valence band to the conduction band, while the TA and the TO phonon couple the Δ_5 valence band to the conduction band and the latter is more efficient for tunneling in the $\langle 100 \rangle$ direction. For germanium, $D_{TA} = 7.8 \times 10^8$ eV/cm and $D_{LO} = 1.3 \times 10^9$ eV/cm and the TA phonon couples the L_3 (Λ_3) valence band to the conduction band, while the LO phonon couples the L_1 (Λ_1) band to the conduction band and the former will be more efficient when tunneling is perpendicular to the $\langle 111 \rangle$ direction. If tunneling is along a direction significantly different from the $\langle 100 \rangle$ direction in silicon and a direction perpendicular to $\langle 111 \rangle$ in germanium, or if valley degeneracy is broken, BTBT assisted by LO phonons will dominate in silicon and germanium.

We acknowledge the support of the Nanoelectronics Research Initiative's (NRI's) Southwest Academy of Nanoelectronics (SWAN).

- ¹A. S. Verhulst, W. G. Vandenberghe, K. Maex, and G. Groeseneken, *Appl. Phys. Lett.* **91**(5), 053102 (2007).
- ²A. M. Ionescu and H. Riel, *Nature* **479**(7373), 329 (2011).
- ³J. Padilla, C. Alper, F. Gámiz, and A. Ionescu, *Appl. Phys. Lett.* **105**(8), 082108 (2014).
- ⁴P. Kerber, Q. Zhang, S. Koswatta, and A. Bryant, *IEEE Electron Device Lett.* **34**(1), 6 (2013).
- ⁵E. Kane, *J. Phys. Chem. Solids* **12**(2), 181 (1960).
- ⁶E. O. Kane, *J. Appl. Phys.* **32**(1), 83 (1961).
- ⁷W. Vandenberghe, B. Sorée, W. Magnus, and M. V. Fischetti, *J. Appl. Phys.* **109**(12), 124503 (2011).
- ⁸K.-H. Kao, A. S. Verhulst, W. G. Vandenberghe, B. Sorée, G. Groeseneken, and K. De Meyer, *IEEE Trans. Electron Devices* **59**(2), 292 (2012).
- ⁹K.-H. Kao, A. S. Verhulst, R. Rooyackers, B. Douhard, J. Delmotte, H. Bender, O. Richard, W. Vandervorst, E. Simoen, A. Hikavyy *et al.*, *J. Appl. Phys.* **116**(21), 214506 (2014).
- ¹⁰C. Rivas, R. Lake, G. Klimeck, W. R. Frensley, M. V. Fischetti, P. E. Thompson, S. L. Rommel, and P. R. Berger, *Appl. Phys. Lett.* **78**(6), 814 (2001).
- ¹¹A. Chynoweth, R. Logan, and D. Thomas, *Phys. Rev.* **125**(3), 877 (1962).
- ¹²R. Logan and A. Chynoweth, *Phys. Rev.* **131**(1), 89 (1963).
- ¹³J.-Q. Wang, Z.-Q. Gu, M.-F. Li, and W.-Y. Lai, *Commun. Theor. Phys.* **20**(2), 159 (1993).
- ¹⁴J. Sjakste, N. Vast, and V. Tyuterev, *Phys. Rev. Lett.* **99**(23), 236405 (2007).
- ¹⁵K. Borysenko, J. Mullen, E. Barry, S. Paul, Y. Semenov, J. Zavada, M. B. Nardelli, and K. Kim, *Phys. Rev. B* **81**(12), 121412(R) (2010).
- ¹⁶K. Kaasbjerg, K. S. Thygesen, and K. W. Jacobsen, *Phys. Rev. B* **85**(11), 115317 (2012).
- ¹⁷G. Kresse and J. Furthmüller, *Comput. Mater. Sci.* **6**(1), 15 (1996).
- ¹⁸W. Vandenberghe and M. Fischetti, in *2014 International Workshop on Computational Electronics (IWCE)* (IEEE, 2014), pp. 1–2.
- ¹⁹J. M. Ziman, *Electrons and Phonons: The Theory of Transport Phenomena in Solids* (Clarendon Press Oxford, UK, 2001).
- ²⁰M. Fischetti and J. Hgman, in *Monte Carlo Device Simulation* (Springer, 1991), pp. 123–160.
- ²¹M. V. Fischetti, J. Kim, S. Narayanan, Z.-Y. Ong, C. Sachs, D. K. Ferry, and S. J. Aboud, *J. Phys.: Condens. Matter* **25**(47), 473202 (2013).
- ²²L. De Lathauwer, B. De Moor, and J. Vandewalle, *SIAM J. Matrix Anal. Appl.* **21**(4), 1253 (2000).
- ²³M. Cardona and F. H. Pollak, *Phys. Rev.* **142**(2), 530 (1966).
- ²⁴M. S. Dresselhaus, G. Dresselhaus, and A. Jorio, *Group Theory* (Springer, 2008).
- ²⁵W. G. Vandenberghe, B. Sorée, W. Magnus, G. Groeseneken, and M. V. Fischetti, *Appl. Phys. Lett.* **98**(14), 143503 (2011).
- ²⁶R. T. Payne, *Phys. Rev.* **139**(2A), A570 (1965).